Plasma protein binding as an optimisable parameter for acidic drugs

Philip Gardiner, Rhona J. Cox, Ken Grime

Clinical Pharmacology & Safety Sciences, Medicinal Chemistry and DMPK,
Respiratory, Inflammation and Autoimmune (RIA), R&D BioPharmaceuticals,
AstraZeneca, Gothenburg, Sweden

Running title: Plasma protein binding as an optimisable parameter for acidic drugs

Address for Correspondence: Philip Gardiner

CPSS, R&D BioPharmaceuticals

AstraZeneca

Pepparedsleden 1, SE-431 83 Mölndal, Sweden

T: +46 (0)31 776 1418

E-mail: philip.gardiner@astrazeneca.com

Text pages: 38

Tables: 3

Figures: 7

References: 55

Number of words in abstract: 165

Number of words in introduction: 576

Number of words in discussion: 1614

Abbreviations: CL, clearance; CL_{int}, intrinsic clearance; $CL_{int,u}$, unbound intrinsic clearance; Cmax, maximum concentration; Cmin, minimum concentration; CXCL8, interleukin-8; CXCR2, CXC chemokine receptor 2; fu_{inc}, fraction unbound in the incubation; IVIVE, in vitro-in vivo extrapolation; LC-MS/MS, liquid chromatography/tandem mass spectrometry; PPB, plasma protein binding; PK, pharmacokinetics; Vss, volume of distribution at steady state; Vss,u volume of distribution at steady state corrected for plasma protein binding.

Abstract

The low volume of distribution associated with acidic molecules means that clearance must also be very low to achieve an effective half-life commensurate with once or twice daily dosing. Plasma protein binding (PPB) should not usually be considered a parameter for optimisation but in the particular case of acidic molecules, raising the PPB above a certain level can result in distribution volume becoming a constant low value equal to the distribution volume of albumin whilst acting to reduce CL through restricting hepatic and renal access of unbound drug. Thus effective half-life can be increased. Here we detail the approaches and lessons learned at AstraZeneca during the optimisation of acidic CXCR2 antagonists for the oral drug treatment of inflammatory diseases, resulting in discovery and clinical testing of AZD5069 and AZD4721, orally bioavailable acidic molecules with PPB of <1%, human hepatocyte intrinsic clearance values < 5 µl/min/10^6 cells and predicted human Vss < 0.3 L/kg, resulting in effective half-lives in man of 4 and 17 h respectively.

Significance Statement

Provided that pharmacological potency is high enough, modulation of plasma protein binding can form part of a viable strategy in drug discovery to optimise effective half-life of drug candidates in humans

Introduction

The delivery of compounds into clinical drug development with optimal pharmacokinetics (PK) is important to overall clinical success (Schuster et al., 2005; Cook et al., 2014) and consequently the ability to accurately predict human PK prior to clinical investment is of high importance (Di et al., 2013). Understanding relationships between pharmacological potency, drug property space and PK, and being able to manipulate these through medicinal chemistry design, lies at the heart of modern drug discovery. This is itself reliant on detailed scrutiny of *in vitro* and *in vivo* drug metabolism and pharmacokinetic (DMPK) data and an awareness of associated caveats (Di et al., 2013; Houston, 2013; Lavé 2009). For acidic compounds the optimisation of PK required for once or twice daily clinical dosing is particularly challenging. The majority of acidic drugs have low steady state distribution volumes (Vss) in the range of 0.1 - 0.3 L/kg (Grime et al., 2013) due to a combination of high plasma protein binding (PPB) and low tissue distribution (Smith and Kerns, 2010) unless active hepatic uptake is a determining factor (Gardiner and Paine, 2011; Grover and Benet, 2009). Drug clearance must therefore also be very low in order to achieve a suitable effective half-life (Bonn et al., 2016; Smith & Kerns 2010). Although PPB should generally not be a parameter for optimisation in drug discovery projects (Smith and Kerns, 2010), in the particular case of acidic molecules, this can be an acceptable strategy. Raising the PPB can result in Vss reaching the lower limiting value of approximately 0.1 L/kg, the distribution volume of albumin (Rowland and Tozer, 1989), and therefore further PPB increases cannot result in lowering of Vss below this value but can reduce CL through restricting access of unbound drug to the hepatocytes. Through impacting CL but not Vss, half-life is increased and Cmax (and therefore dose) is reduced if the aim is to maintain free drug concentrations above a fixed

DMD Fast Forward. Published on May 21, 2019 as DOI: 10.1124/dmd.119.087163

minimum effective drug concentration. This strategy for optimizing acidic drugs can work if there is excellent pharmacological potency allowing efficacious free blood levels to be maintained at target receptors (Grime and Riley 2006). With these concepts in mind it is interesting to note that in an earlier review of the relevant literature we found that, of the 9 examples of marketed oral acidic drugs with half-lives of more than 8 h, 7 of these have plasma protein binding of ≥ 99% (naproxen, piroxicam, atovaquone, diflunisal, cetirizine, warfarin and oxaprozin (Grime et al., 2013).

The CXC chemokine receptor 2 (CXCR2) is expressed on the surface of neutrophils and is involved in the recruitment of these phagocytic white blood cells to sites of inflammation through CXCL8 (interleukin-8, IL-8) signalling (Mukaida 2003). Accordingly, antagonism of CXCR2 has been proposed as a strategy for the treatment of inflammatory diseases such as arthritis, chronic obstructive pulmonary disease and cancer (Holmes et al., 1991; Murphy et al., 1991; Beeh et al., 2003; Jamieson et al., 2012; Highfill et al., 2014, Steele et al., 2016).

In the AstraZeneca CXCR2 drug discovery program, the acidity of the molecules was shown to be an important parameter for increasing both CXCR2 receptor binding and PPB (Austin et al., 2015). This manuscript outlines the approaches taken and lessons learned from early CXCR2 clinical drug candidates and describes the pre-clinical data analysis that led to a strategy for achieving PK half-lives commensurate with once and twice daily dosing, ultimately resulting in the improved clinical drug candidates AZD5069 and AZD4721.

Materials and Methods:

Chemicals. All chemicals and reagents used were of the highest available grade. The AstraZeneca compounds including AZD5069 and AZD4721 were synthesised in house by AstraZeneca (Austin et al., 2000; Willis et al., 2001; Ebden et al., 2004; Bonnert, 2004; Brough et al., 2005; Cheshire et al., 2006; Connolly et al., 2013). All other chemicals were purchased from Sigma-Aldrich (Poole, Dorset, UK). Hepatocyte suspension buffer was prepared from powder-equivalent Dulbecco's modified Eagle's medium (Sigma, Gillingham, UK) containing Na HEPES (2.34 g) and D-fructose (0.4 g) in 1 L of Milli-Q® water. The pH was adjusted to be 7.4 with HCl (1M) at 37°C. Hepatocyte suspension buffer contained bovine serum albumin (BSA, 2 g) to wash cells after the hepatic isolation procedure, but intrinsic clearance incubation buffer was prepared without BSA.

Hepatocyte preparations. Rat hepatocytes were isolated from male Sprague-Dawley rats using the two-step *in situ* collagenase perfusion method of Seglen (1976) described previously (Soars et. al. 2007). Dog hepatocytes were isolated in house from male beagle dogs of approximately 1 year old. The isolation procedure was based on the two-step *in situ* collagenase perfusion method described in more detail previously (McGinnity et al. 2004). Rat and dog hepatocytes were re-suspended for assay use in suspension buffer without BSA and viability was assessed using the trypan blue exclusion method. Only cells with a viability >80% were used. Cryopreserved isolated human hepatocytes were obtained from CellzDirect Inc (Durham, NC, USA) and thawed according to supplied instructions.

Equilibrium dialysis measurement of plasma protein binding (PPB). This was performed as previously described (Fessey et al., 2006). In summary, to one compartment of each of the dialysis cells were added 1 mL of plasma and 10 μL of a solution of compound at a concentration of 2 mM in DMSO. The second section of each dialysis cell was filled with 1 mL phosphate buffer (pH 7.4, 0.1 M). The cells were then sealed, attached to the Dianorm unit, and rotated in a water bath at 37 °C for 18 h. Plasma (100 µL) from the dialysis cell was added to phosphate buffer (500 µL) and 500 µL of the buffer solution from the dialysis cell was pipetted in to blank plasma (100 µL). The samples were analysed using HPLC with MS detection. Due to the frequent non-linear response of mass spec. detectors, a calibration curve was obtained from dilutions of the stock solutions with 6-fold diluted plasma. The concentrations of the four standards were 0.05 µM, 0.15 µM, 0.5 µM, 2.5 µM and injected in this order followed by the buffer samples and then the plasma samples. The extent of PPB was calculated as described by Fessey et al. (2006). The chromatogram peak areas were processed automatically to use the calibration curve for each compound to calculate the concentration of unknowns. These “concentrations” were corrected for differences in injection volumes and the dilution of the plasma. The percentage bound value was calculated using the following equation:

$$\%\, Bound = 100 - 100\left(\frac{1.2\left(\frac{buffer\ concentration\ x\ standard\ injection\ volume}{buffer\ injection\ volume}\right)}{6\left(\frac{plasma\ concentration\ x\ standard\ injection\ volume}{plasma\ injection\ volume}\right)}\right)$$

The factor of 1.2 in the numerator accounts for the small dilution of the aqueous samples with plasma. The factor of 6 in the denominator serves to correct for the 6-fold dilution of the plasma samples with buffer.

Each compound was measured in duplicate in the same experiment. The precision of the assay was assessed over many duplicate measurements performed across structurally diverse compounds. Table 1 contains the ratio of % free for duplicate pairs of measurements from the same batch of plasma for 1681 compounds measured in the protein binding assay. The distribution of duplicate pair-ratios was almost normally distributed, and applying the assumption of normality, it can then be calculated that 95% of duplicate ratios are less than 2.14. Any duplicate ratio larger than 2.14 is therefore a rare occurrence and can be termed an outlier, and the assay would be repeated for this compound.

Table 2 contains mean free % ratios when the same compound was measured on different days i.e. with a different batch of plasma. The mean % free on one day (mean of 2 data points) was then compared with the mean % free on another day for each compound.

The data in Table 2 show that the average ratio of the mean % free determined one day to the mean % free determined on another day is about 1.5, with a standard deviation (SD) of about 0.5. The SDs in Table 2 are not directly comparable with the SDs in Table 1 since the SDs in Table 2 are the average standard deviation of the ratio of two means (each a mean of 2 data points), whereas the SDs in Table 1 are the average standard deviation of the ratio of 2 single measurements of % free. The 95% limit for duplicate ratios in Table 2 indicates that if a compound is measured on 2 different days and the mean % free differs by a factor of greater than about 2.6, then the data must be viewed as suspect (even if each of the two duplicates has a satisfactory duplicate ratio), and more experiments should be carried out. Hence, during the discovery phase when comparing the % free of different compounds, the assay performance analysis indicated that for compounds measured once (in duplicate), a difference between compounds ≥ 2.6 in the fu was required to be judged a significantly different %free value at the 95% level. In general, compounds were tested on two separate occasions and key compounds such as AZD5069 and AZD4721 on 5 or more occasions.

Determination of blood-plasma ratio (B:P). Stock concentrations of test compounds were 100-fold above final incubation concentrations and these were pipetted into fresh blood and plasma (0.5 mL). After 15 minutes incubation (37ºC) and centrifugation (9000g, 4 minutes) using an MSE MicroCentaur® centrifuge (Fisher Scientific, Loughborough, UK), aliquots from both the blood and plasma incubations were pipetted into methanol and stored at –20ºC for one hour. Samples were centrifuged (2000g, 20 minutes) and the supernatant analysed by LC-MS/MS. B:P was calculated from the ratio of the analyte concentration in directly spiked plasma to that in plasma isolated from spiked blood. Key compounds such as AZD5069 and AZD4721 were tested across species

Measurement of logD$_{7.4}$, pKa and solubility. For logD$_{7.4}$ determination, separation of compounds between 1-octanol and phosphate buffer (0.02 M, pH 7.4 at 20°C) was determined using a shake flask method (Leo et al., 1971). Octanol and aqueous tiers were analyzed by LC-MS/MS as described below. pKa was measured using a Sirius GLpKa instrument with DPAS (Dip Probe Absorption Spectroscopy) attachment (Sirius Analytical Instruments Ltd). Samples of test compounds were placed in vials in a movable autosampler tray for titration. Assays were set up using the GlpKaControl software and results analysed using the pKaLOGP and pKaUV software which allows determination of multiple pKas using complex curve fitting analyses. Solubility was measured as described previously (Wenlock et al., 2011b). In brief, compounds (1 mg) were placed into separate 2 mL glass tubes and phosphate buffer (pH 7.4, 0.1 M, 1 mL) added. The vials were shaken for a minimum of 18 h. After shaking, the saturated solutions were transferred to 2 mL centrifuge tubes and centrifuged at 13000g for 15

DMD Fast Forward. Published on May 21, 2019 as DOI: 10.1124/dmd.119.087163

minutes. The supernatants were then removed, placed into new centrifuge tubes, and centrifuged again at 13000g for 15 minutes. Aliquots of the supernatants from the second centrifugation were analysed by LC-MS/MS along with standard concentration stock solutions, prepared by adding DMSO (800 µL) to compound (1 mg) and sonicating (15 minutes). Single measures were generally regarded as sufficient except for key compounds such as AZD5069 and AZD4721.

Determination of intrinsic clearance. Test compound stock solutions were prepared in DMSO at 100-fold incubation concentration (100 µM). Stock solution (10 µL) was added to hepatocyte suspension buffer (490 µL). This solution and separately hepatocytes (2 million viable cells/mL) were pre-incubated for 5 minutes in a shaking (80 oscillations/minute) water-bath at 37°C. Reactions were initiated by adding hepatocyte suspension (500 µL) to test compound solution giving a final substrate concentration of 1 µM and 1% (v/v) DMSO. Aliquots (40 µL) were removed at 0, 2, 6, 15, 30, 45, 60, and 90 minutes and reactions were quenched in 120 µL of ice-cold methanol. Samples were subsequently frozen for 1 h at -20°C and then centrifuged at 2000g for 20 min at 4°C. The supernatants were removed for LCMS/MS analysis. Analytical LC-MS/MS peak areas of samples were $\log_e$-transformed and elimination rate constants k (min^{-1}) were derived from the slopes of the $\log_e$[substrate]-time plots. Intrinsic clearance was calculated from CL_{int},= k x V, where V represents the incubation volume (mL/mg protein or mL/million cells). Key compounds such as AZD5069 and AZD4721 were incubated on at least 3 separate occasions in rat, dog and human hepatocytes.

Methods for prediction of hepatic metabolic CL. Clearance predictions were made using a ‘regression line approach’, whereby an existing *in vitro-in vivo* unbound CL_{int} dataset (for which *in vivo* CL_{int} values represent metabolic clearance only) is used as a framework for predicting the *in vivo* clearance for novel compounds (Sohlenius-Sternbeck et al., 2012). However, determination of whether the clearance of a compound is well predicted from the *in vitro* data comes from the assessment of $CL_{int,u\ in\ vivo}$ / $CL_{int,u\ in\ vitro}$ which should be between 0.5 and 2 (Grime et al., 2013). See Table 3 for AZD5069 and AZD4721 predictions.

Preclinical *in vivo* studies. All *in vivo* work was subject to internal ethical review and conducted in accordance with UK Home Office requirements under the Animals Scientific Procedures Act (1986). Healthy virus antibody-free male Sprague Dawley rats were obtained from Charles River (Margate, UK). They were housed in a light-controlled room (19°C ± 2°C and 55% ± 10% humidity). A Teklad 2021 diet (Harlan) was used with drinking water ad libitum. In-house bred male beagles (housed in pairs, temperature of 18°C ± 2°C and humidity 55% ± 10%) were fed with a SDS D3 (E) Dog Maintenance diet with water ad libitum.

Intravenous and per os (PO) pharmacokinetic studies. *Rat*: AZD5069 and AZD4721 were dosed at 1 mg/kg as a bolus to the tail vein in DMA:H_20 (1:9 v/v) to conscious male rats (n=3 or 4). PO doses were given via oral gavage in a Tween (0.1%) Hydroxypropyl methylcellulose (HPMC) (1%) suspension (n=3). Serial blood samples (200–300 µL) were taken and plasma recovered after centrifugation.

Dog: AZD5069 and AZD4721 were dissolved in bicarbonate buffer (pH 10) including 10% ethanol to a concentration of 1 mg/mL. The dose was given via infusion (30 minutes) to the cephalic vein. PO doses were given via oral gavage in a Tween (0.1%) HPMC (1%) suspension (n=2). Serial blood samples (2.5 mL) were taken and centrifuged to obtain plasma.

Intravenous bile duct cannulation (BDC) studies (AZD5069 and AZD4721). *Rat:* After at least 1 week of acclimatisation rats (250-350 g) were surgically prepared under

DMD Fast Forward. Published on May 21, 2019 as DOI: 10.1124/dmd.119.087163
This article has not been copyedited and formatted. The final version may differ from this version.

isoflurane anaesthesia. The bile duct was cannulated with a bile-pancreatic catheter (constructed by polyethylene catheter Physiocath and P90; Data Sciences International, St. Paul, MN). An opening was made in the duodenum and the catheter inserted for bile re-circulation. A small cut in the skin (around the area of the scapula) facilitated subcutaneous routing of the catheter. After 3 days' recovery, the animals were connected to a swivel system (Instech Laboratories, Plymouth Meeting, PA) that allowed freedom of movement during the experiment. Cannulae were inserted into the jugular and carotid blood vessels for dosing and blood sampling respectively. A bile sample was taken over the first hour post dosing and then every half hour until 7 h.. Blood samples (200–300 µL) were taken at the midpoint of the bile collections and plasma prepared as stated above. Urine was also collected and all samples, were stored at -20°C.

Dog: After at least 4 weeks of acclimatisation, a bile duct cannulation (BDC) operation was performed on two dogs following the technique described by Kissinger and Garver (1998). A one month recovery period followed before the study. AZD5069 and AZD4721 were dissolved in bicarbonate buffer (pH 10) including 10% ethanol to a concentration of 1 mg/mL. The dose was given via infusion (30 minutes) to the cephalic vein. Jugular vein sampling of blood (2.5 mL) was made into EDTA-containing tubes at 0, 15, 30, 60, 120, 180, 300, 420, 720 and 1440 minutes post infusion start prior to centrifugation (1110g, 10 minutes) for plasma collection. Bile and urine collection continued for 24 h. All samples were stored at -20°C prior to analysis.

Sample Preparation: Prior to analysis, samples from the *in vivo* studies were prepared as follows: Aliquots (50 µL) of plasma were added to methanol (150 µL). Water was added to the bile and urine before analysis. Standard curves and quality control (QC samples) were made up in matrix blanks.

Sample analysis. Samples were analysed by LC-MS/MS (HP1100 HPLC system supplied by Hewlett Packard, Quattro Ultima mass spectrometer supplied by Micromass, Waters, Milford, MA, USA). Electrospray ionization mode was used. For HPLC a Waters Symmetry C8 3.5 µm (2.1 x 30 mm) column was utilized injecting 10 µL of each sample. Mobile phase was water plus 0.1 % formic acid and methanol plus 0.1 % formic acid.

Pharmacokinetics. Parameters (clearance, Vss, and terminal half-life) were derived from the concentration-time profile by non-compartmental analysis using WinNonlin® Professional Version 5.2 (Pharsight Corporation, Mountain View, CA). Clearance estimated as dose divided by AUC where AUC is the area under the concentration-time curve from time zero extrapolated to infinity. AUC is estimated by AUC(0-last) + Clast/λz where Clast is the last observed quantifiable concentration. Vss was estimated by dividing the Mean Residence Time by the clearance. Terminal half-life, was estimated as (ln2)/λz, where λz is the terminal rate constant, estimated by log-linear least squares regression of the terminal part of the concentration-time curve.

Prediction of human Vss and effective half-life. The average of rat and dog Vss,u (Vss adjusted for PPB) was used to predict human Vss,u, which was then multipled by human PPB to predict human Vss. Human effective half-life was predicted from 0.693 x predicted Vss / predicted CL.

Metabolite identification studies. *In vitro* incubations were performed with isolated rat, dog and human hepatocytes (2 million cells/mL). AZD5069 and AZD4721 (10 µM) were incubated for 1 hour at 37°C. The incubations were quenched with two volumes of methanol, vortexed and stored at -20°C. Samples were prepared just prior to MS analysis by centrifugation at 9000g for 30 minutes and transferring the supernatant to sample vials. *In vivo* samples were prepared as follows: urine and bile samples were diluted 1 part bile or urine to 1 part methanol, vortexed and frozen. Plasma samples were quenched with 3 volumes of methanol and frozen. Samples were defrosted, vortexed and centrifuged (9000g for 30 minutes) just before analysis and the supernatant taken and diluted 1:1 with water. Samples were analysed in positive ion mode. The MS method used consisted of two MS channels, a normal MS scan and a source induced decomposition (SID) channel to provide structural data on parent compound and metabolites. Where necessary, MSMS was also carried out. All MS data was acquired with a mass accuracy of 5 ppm. After the analysis, the data was processed manually to identify the major metabolites based on MS response. Minor metabolites were defined as representing ≤1% of the total response.

Clinical PK. Both the AZD5069 and AZD4721 studies were approved by an Independent Ethics Committee prior to initiation and were performed in accordance with the ethical principles that have their origin in the Declaration of Helsinki and that are consistent with International Conference on Harmonisation/Good Clinical Practice, applicable regulatory requirements and the AstraZeneca Policy on Bioethics. Informed consent was obtained from all volunteers prior to initiation of the studies. AZD5069 human pharmacokinetic data was generated in a phase I, blinded, randomised, placebo-controlled, single-centre study (NCT00953888 and Cullberg et. al. 2018) to investigate the safety, tolerability, pharmacokinetics, and pharmacodynamics of oral AZD5069 after single ascending doses in Caucasian male and female healthy volunteers with body mass indices between 18 and 30 kg/m^2 (inclusive) and weights between 50 and 100 kg (inclusive). The study was performed at AstraZeneca Clinical Pharmacology Unit, Queens Medical Centre, Nottingham NG7 2UH. Serial blood samples were taken up to 96 h post dose and plasma samples were analysed using validated bioanalytical methods at AstraZeneca R&D Charnwood. PK parameters were derived using standard non-compartmental methods. AZD4721 human pharmacokinetic data was generated in a separate phase 1, blinded, randomised, placebo-controlled, single-centre study (NCT01889160) to investigate the safety, tolerability, pharmacokinetics, and pharmacodynamics of oral AZD4721 after single ascending doses in Caucasian male healthy volunteers with body mass indices between 18 and 30 kg/m^2 (inclusive) and weights between 50 and 100 kg (inclusive). The study was performed at Quintiles Drug Research Unit at Guy’s Hospital London, England. Serial blood samples were taken up to 216 h post dose and plasma samples were analysed using validated bioanalytical methods and pharmacokinetic parameters were derived using noncompartmental methods with WinNonlin® Professional Version 5.2, or higher, (Pharsight Corp., Mountain View, CA).

Data Analysis

Impact of PPB on rat pharmacokinetics. *In vivo* rat CL was plotted against rat PPB data and separately rat Vss, for the thiazolone and sulfamide chemical series investigated in the CXCR2 program.

Simulating the impact of PPB on human half-life. The CL prediction method (using the ‘regression line approach’ and unbound *in vivo* and *in vitro* CL$_{int}$, see Methods above) was used to calculate CL at various values of PPB when human hepatocyte CL$_{int}$ was of 1 µL/min/ million hepatocytes. Changes in half-life were calculated as 0.693 x Vss / CL when Vss was constant at 0.2 L/kg (unaffected by plasma protein binding).

DMD Fast Forward. Published on May 21, 2019 as DOI: 10.1124/dmd.119.087163
This article has not been copyedited and formatted. The final version may differ from this version.

Results

Analysis of the impact of plasma protein binding on rat pharmacokinetics.

Plasma protein binding was shown to relate to rat clearance for two chemical series of compounds, thiazolones and sulfamides (Figures 1 and 2A). Vss was found to be low, as expected for acidic molecules, with 70% of the molecules having Vss less than 0.4 L/kg (Figure 2B). The data indicates the lack of a relationship between plasma protein binding and distribution volume.

Simulating the impact of plasma protein binding on human half-life.

Based on the observations in Figure 2, a simple simulation was performed assuming Vss to be typically low for an acidic molecule and constant at 0.2 L/kg. Assuming that it is possible to keep hepatic intrinsic clearance of unbound drug constant whilst increasing PPB, the prediction demonstrates that PPB influences half-life through reducing clearance and indicates that PPB in excess of 99.2% could achieve a half-life in excess of 15 h (Figure 3).

Pre-clinical data and human PK predictions

A summary of key pre-clinical *in vitro* and *in vivo* data for AZD5069 and AZD4721 is shown in Table 3.

AZD5069

Analysis of rat PK data showed that bile duct cannulation had no discernible effect on the PK profile (Figure 4). Subsequent to the readout of the clinical PK data for AZD5069, a BDC study revealed the dog PK profile to have a lower exposure and shorter observed terminal phase than from the non-canulated IV PK experiment, even though biliary clearance of parent AZD5069 was measured as 0.1 mL/min/kg (1.4% of total CL).

AZD4721

As with AZD5069, human CL was predicted to be driven entirely by hepatic metabolism. With lower human hepatocyte CL_{int} and higher human PPB, the effective human half-life was predicted to be considerably longer than that predicted for AZD5069. Unlike AZD5069, dog IV and BDC PK profiles for AZD4721 were very similar in shape and absolute concentration throughout the sampled interval (Figure 5).

Biotransformation data

AZD5069

AZD5069 metabolism was complex, with multiple pathways observed in rat, dog and human. However, the major pathways identified were direct glucuronide conjugation at the diol group, *S*-debenzylation (loss of the methylene-difluorophenyl moiety) and oxidations on the azetidine ring (Figure 6). Qualitatively, the metabolites were generally similar in each of the species but there were quantitative differences, partly as a result of different metabolic turnover rates. The most substantial difference was observed in the dog with the *O*-glucuronide of AZD5069 being by far the most prominent metabolic route and representing 99% of MS response (absolute configuration as an *O*-glucuronide on the 4-hydroxy position of the 3,4-dihydroxy-2-yloxy side chain of AZD5069 was later determined by NMR, *data not shown*).

AZD4721

A similar metabolism pattern to AZD5069 was observed for AZD4721. However, azetidine oxidation products were more minor than for AZD5069, possibly due the addition of the methyl at the azetidine 3-position as well as lower turnover rates in hepatocytes. As with AZD5069, the *O*-glucuronide was the major metabolite observed in dog *in vitro* and *in vivo*, but rather than representing 99% of drug related MS response observed for AZD5069 this was reduced to 56%. From incubations with human hepatocytes, formation of a carboxylic acid metabolite represented 4% of drug related MS response and this was more major than in the either of the other two species or for that observed with AZD5069 (Figure 6).

Clinical PK

AZD5069

Exposure of AZD5069 (AUC and C_{max}) was found to be approximately dose proportional after dosing of 0.1 to 200 mg with an effective half-life of 4 h. The 24 h plasma profile for the 120 mg dose is shown in Figure 7.

AZD4721

AZD4721 geometric mean effective half-life ranged from 14 h to 19 h across the dose range studied (19 to 730 mg) and AUC and C_{max} increased in proportion to the dose. The 24 h plasma profile for the 150 mg dose is shown in Figure 7.

Discussion

The modulation of physicochemical properties to manipulate PK parameters lies at the heart of effective drug discovery (Riley et al., 2002; Davis and Riley, 2004; Di et al., 2013; Lombardo et al., 2014). Indeed, optimizing molecular properties such as size, lipophilicity and polarity has been directly linked to greater success in clinical drug development (Waring et al., 2015).

Early CXCR2 antagonists in the AstraZeneca program had bicyclic thiazolone cores and were relatively lipophilic weak acids with poor solubility (Walters et al., 2008) but nonetheless their properties were sufficiently promising for the lead compound AZD8309 (Figure 1) to be taken into the clinic. Although AZD8309 proved a valuable tool compound to investigate the role of CXCR2 antagonists in inflammatory lung disease (Virtala et al., 2011; Leaker et al., 2013) its PK properties, exemplified by variable human bioavailability and a short half-life, were regarded as unsuitable for further clinical development. In the main these molecules had high PPB, high *in vitro* metabolic instability and low incubational binding which gave poor predictions of *in vivo* rat and dog CL when using a simplified version of the well stirred model, ignoring drug binding terms. These observations and those of others (Iwatsubo et al., 1997; Houston and Carlile 1997; Carlile et al., 1999; Ito and Houston, 2005) gave us greater appreciation of the impact of drug binding on CL predictions and revised CL prediction models resulting from our experiences were subsequently published (Grime and Riley, 2006).

In order to design a CXCR2 antagonist with improved human PK properties, we needed to both improve the bioavailability of AZD8309 and increase the effective half-life. The former was achieved by designing a monocyclic series of sulfamides with increased solubility (Austin et al, 2015). The latter was tackled by examining the data presented in Figure 2A, with the striking observation that a compound could have high metabolic instability and yet low CL *in vivo* if PPB was high enough. Since PPB appeared to have little relationship to distribution volume (Figure 2B), this indicated that half-life could possibly be extended by raising PPB. Theoretically, increasing binding to blood components should reduce distribution of a drug into body tissues (Smith and Kerns, 2010) but this was not observed in the data presented in Figure 2B, most likely due to a combination of poor distribution properties for these acidic molecules and lipophilicity playing a ‘cancelling out’ role through impacting both PPB and affinity for tissue. Given the observation that increasing acidity related to increasing potency and PPB (Austin et al., 2015), the proposed strategy in the CXCR2 program was to increase acidity in order to increase both parameters whilst reducing $\log D_{7.4}$ to obtain better metabolic stability. Using a CL prediction method incorporating drug binding terms and a regression line method (Grime and Riley, 2006; Sohlenius-Sternbeck et al., 2012), a simple simulation demonstrated the general PK strategy for the program (Figure 3).

Eventually this approach led to the discovery of AZD5069 (Figure 1) with the substitution of nitrogen-linked for oxygen-linked pyrimidine playing a major part in giving acceptable lipophilicity, increased acidity and the desired combination of potency, PPB, solubility and metabolic stability (Cheshire et al., 2010, Kärrman Mårdh et al, 2015). The use of an azetidine proved valuable in minimizing metabolism on the left hand side of the molecule, as others have found (Obach et al., 2016) and the diol

DMD Fast Forward. Published on May 21, 2019 as DOI: 10.1124/dmd.119.087163
This article has not been copyedited and formatted. The final version may differ from this version.

provided both reduced $\log D_{7.4}$ and reduced CL_{int} compared to the equivalent mono-alcohols.

AZD5069 had a short half-life in rat and dog but with CL apparently driven solely by metabolism (Table 3). However, with good *in vitro*-*in vivo* extrapolation (IVIVE) for unbound hepatic metabolic CL_{int} (*in vivo* / *in vitro* unbound CL_{int} ratios of between 0.76 and 1.1 for rat and dog, Table 3) there was confidence in achieving the 7.5 h predicted human effective half-life.

Consensus opinion has converged on a definition for accuracy of clinical PK parameter prediction being observed/predicted within twofold (Lave et al., 2009). For AZD5069, the two-fold over-prediction of half-life may not technically be considered failure, but in the context of a 7.5 h predicted half-life being realized as a 4 hour half-life, it represented a complication to the program since once daily dosing was a primary objective. The fact that the effective half-life of AZD5069 after IV dosing was only 1 hour in rat and dog PK studies and yet human half-life was predicted to be almost 8-times longer but was in fact only 4-times longer after PO dosing, prompts useful reflection on the value of allometry based predictions. It has been noted previously that whilst standard allometric scaling approaches offer fairly poor predictivity of human CL (Ward and Smith, 2004; Caldwell et al., 2004), the work of Ward and Smith highlights that human effective half-life often approximates to 4 times rat half-life, offering a useful validation of IVIVE based predictions that should be investigated thoroughly before clinical drug development (Grime et al., 2013). Considerations of the pros and cons of allometric approaches are discussed in detail elsewhere (Di et al., 2013), but discrepancies between allometric and IVIVE predictions can come from species differences in PPB, drug metabolising enzyme or drug transporter kinetics. As with all candidate drugs at AstraZeneca, the checks used for AZD5069 included an assessment linearity of *in vitro* intrinsic clearance with respect to drug concentration, based on the work of Obach and Reed-Hagen (2002) and that for human hepatic microsomal and hepatocyte intrinsic clearance data gave consistent predictions of hepatic clearance.

In attempting to understand what may have caused the discrepancy between predicted and observed effective human PK half-life, attention was drawn to the larger Vss in dogs compared to rats and the longer terminal half-life, in comparison to the effective half-life, in the dog PK profile (Figure 4). This PK profile feature is quite unusual for an acidic drug with inherently poor distribution properties. A BDC study in dog revealed the PK profile to have a lower exposure and shorter observed terminal phase than from the non-cannulated IV PK experiment, indicating possible enterohepatic recirculation. However, AZD5069 biliary clearance was measured as being similarly low (0.1 and 0.1 mL/min/kg representing 1.5 and 2 % of total CL) in rats and dogs respectively. Metabolite identification data from *in vitro* (dog hepatocyte incubations) and *in vivo* samples (urine and bile analysis from the IV dosed dog BDC experiment) highlighted direct glucuronidation of the secondary alcohol as the major metabolite seen in dog. In comparison, the glucuronide metabolite was less prominent in the rat *in vivo*, or rat and human *in vitro* samples, for which oxidation (of the alcohols, at the *S*-benzyl position and on the azetidine ring) were also observed as principal metabolites (Figure 6). Taken together, these data suggest that enterohepatic recirculation, involving biliary excretion of hepatically formed *O*-glucuronide metabolites followed by intestinal hydrolysis to the aglycone parent AZD5069 with subsequent re-absorption, may have extended the observable terminal PK phase in the standard IV dog PK experiment leading to over-estimation of predicted Vss and effective half-life, as has been observed previously (Ouellet and Pollack 1995; Deng et al., 2012).

Despite AZD5069 being a very attractive drug for twice daily dosing, we still had an ambition to design a once daily drug. There was still belief in the strategy of raising human PPB to improve half-life, and through subtle structural changes AZD4721 (Figure 1) was designed. The changes that achieved these improvements were methylation of the azetidine and replacement of the 2,3-difluorobenzyl with a 4-fluorobenzyl group. In fact, an increase in PPB giving a decrease in blood free fraction of almost 6-fold was achieved for AZD4721 in comparison to AZD5069, despite almost identical $\log D_{7.4}$ and pKa values (Table 3). Metabolic stability was also slightly improved, with a mean HLM CL_{int} value approaching two-fold lower for AZD4721. AZD4721 was also primarily metabolised by direct glucuronidation in dogs, with a qualitatively very similar metabolic map to that of AZD5069 in all species. However, with lower intrinsic clearance and greater than ten-fold lower *in vivo* CL, enterohepatic recirculation was not observed in the AZD4721 dog PK profile in the sampled interval and therefore had no impact on estimated Vss. Given the uncertainty around the predicted and observed human Vss for AZD5069, as discussed above, Vss for AZD4721 was set to the lower limiting value of 0.1 L/kg (Rowland and Tozer, 1989) in making the predictions of human PK. Clinical data for AZD4721 confirmed that the strategy of increasing plasma protein binding for acidic drugs can be successful in reducing clearance to very low levels and therefore providing an effective half-life long enough for once daily dosing with minimal C_{max}/C_{min}, despite very low distribution volume (Figure 7). An alternative or complimentary approach can be to increase the blood to plasma ratio through drug binding to erythrocyte components. One example of this is to use the affinity of primary sulphonamides for the carbonic anhydrase enzyme (Boddy et al., 1989). Of course, for such a molecule to be an effective therapeutic drug requires at least that the pharmacological potency is high enough at a deliverable dosage to overcome the issue of low free fraction in blood. The *in vitro* potency properties and sustained clinical profile of AZD4721 indicated that this should not be an issue in this case. Even though the observed half-life was 1.6-fold less than predicted, the fact that the predicted half-life approximated to the required dose interval minimised the relevance of this.

In summary, this work details the optimisation strategy of acidic CXCR2 antagonists, resulting in two molecules, AZD5069 and AZD4721, suitable for twice and once daily oral dosing respectively, and shows that under certain circumstances, optimisation of binding to plasma proteins can be a viable strategy to optimise effective half-life in humans.

Acknowledgements

Steve Connolly, Alison Wilby, Rob Riley, Jane Kenny, Anthony Atkinson, Premji Meghani, Jeffrey Stonehouse, Roger Bonnert, David Cheshire, Iain Walters, Mark Ebden, Alasdair Gaw, Andy Davis, Rupert Austin, Marie Cullberg, Bengt Larsson, Heather Wray, Anna Malmgren.

Authorship Contributions

Participated in research design: Gardiner, Cox and Grime.

DMD Fast Forward. Published on May 21, 2019 as DOI: 10.1124/dmd.119.087163

Conducted experiments: Gardiner, Cox and Grime.

Performed data analysis: Gardiner; Cox and Grime.

Wrote or contributed to the writing of the manuscript: Gardiner; Cox and Grime

DMD Fast Forward. Published on May 21, 2019 as DOI: 10.1124/dmd.119.087163
This article has not been copyedited and formatted. The final version may differ from this version.

References

Austin R, Baxter A, Bonnert R, Hunt F, Kinchin E, Willis P (2000) Novel thiazolopyrimidine compounds. Patent number: WO200009511 A1.

Austin RP, Bennion C, Bonnert RV, Cheema L, Cook AR, Cox RJ, Ebden MR, Gaw A, Grime K, Meghani P, Nicholls D, Phillips C, Smith N, Steele J, Stonehouse (2015) Discovery and evaluation of a novel monocyclic series of CXCR2 antagonists. *Med Chem Lett* 1;25(7):1616-20.

Beeh KM, Kornmann O, Buhl R, Culpitt SV, Giembycz MA, Barnes PJ (2003) Neutrophil chemotactic activity of sputum from patients with COPD: role of interleukin 8 and leukotriene B4. *Chest* 123: 1240–1247.

Boddy A, Edwards P, Rowland M. (1989), Binding of sulfonamides to carbonic anhydrase: influence on distribution within blood and on pharmacokinetics. *Pharm Res.* 6(3):203-209.

Bonn B, Svanberg P, Janefeldt A, Hultman I, Grime K (2016) Determination of human hepatocyte intrinsic clearance for slowly metabolized compounds: comparison of a primary hepatocyte/stromal cell co-culture with plated primary hepatocytes and HepaRG. *Drug Metab Dispos* 44(4): 527-33.

Bonnert RV (2004) Novel compound. Patent number: WO2004026880 A1.

Brough SJ, McInally T (2005) Novel compound. Patent number: US20050272750 A1.

Carlile DJ, Hakooz N, Bayliss MK, Houston JB. (1999) Microsomal prediction of in vivo clearance of CYP2C9 substrates in humans. *Br J Clin Pharmacol* 47(6): 625-635.

Cheshire DR, Cox RJ, Meghani P, Preston CF, Smith NM, Stonehouse JP (2006) Pyrimidine sulphonamide derivatives as chemokine receptor modulators. Patent number: WO2006024823 A1.

Cheshire DR, Cox RJ, Meghani P, Stonehouse JP. (2010) Pyrimidine sulphonamide derivatives as chemokine receptor modulators. Patent number: US7838675 B2.

Connolly S, Ebden MR, Langer T, Steven AR, Stewart CR, Tomlin PM, Walters IAS, Williams AJ (2013) N-(6-((2R,3S)-3,4-Dihydroxybutan-2-yloxy)-2-(4-fluorobenzylthio)pyrimidin-4-yl)-3-methylazetidine-1-sulfonamide as chemokine receptor modulator. Patent number: WO2013008002 A1.

Cook D, Brown D, Alexander R, March R, Morgan P, Satterthwaite G, Pangalos MN (2014) Lessons learned from the fate of AstraZeneca's drug pipeline: a five-dimensional framework. *Nat Rev Drug Discov* 13(6): 419-31.

Cullberg M, Arfvidsson C, Larsson B, Malmgren A, Mitchell P, Hamrén UW, Wray H (2018) Pharmacokinetics of the oral selective CXCR2 antagonist AZD5069: a summary of eight phase I studies in healthy volunteers *Drugs R D.* 18(2): 149-159.

Davis AM, Riley RJ. (2004) Predictive ADMET studies, the challenges and the opportunities. *Curr Opin Chem Biol* 8(4): 378-386.

Deng J, Zhuangy X, Shen G, Lin H, Gong Z (2012) Biliary excretion and enterohepatic circulation of thienorphine and its glucuronide conjugate in rats. *Acta Pharmaceutica Sinica B* 2(2): 174–180.

Di L, Feng B, Goosen TC, Lai Y, Steyn SJ, Varma MV, Obach RS. (2013), A perspective on the prediction of drug pharmacokinetics and disposition in drug research and development. *Drug Metab Dispos* 41(12): 1975-1993.

Ebden MR, Meghani P, Bennion C, Cook AR, Bonnert RV (2004) Pyrimidyl sulphone amide derivatives as chemokine receptor modulators. Patent number: WO2004011443 A1.

Fessey RE, Austin RP, Barton P, Davis AM, Wenlock MC, The role of plasma protein binding in drug discovery, in: B. Testa, S.D. Kramer, H. Wunderli-Allenspach, G. Folkers (Eds.), Pharmacokinetic Profiling in Drug Research: Biological, Physicochemical, and Computational Strategies, Wiley-VCH, Weinheim, 2006, pp. 119–141.

Gardiner P, Paine SW (2011) The impact of hepatic uptake on the pharmacokinetics of organic anions *Drug Metab Dispos* 39: 1930– 1938.

Grime K, Riley RJ (2006) The Impact of In Vitro Binding on In Vitro - In Vivo Extrapolations, Projections of Metabolic Clearance and Clinical Drug-Drug Interactions *Curr Drug Metab* 7: 251– 264.

Grime KG, Barton P, McGinnity DF (2013) Application of In Silico, In Vitro and preclinical pharmacokinetic data for the effective and efficient prediction of human pharmacokinetics. *Mol Pharmaceutics* 10 (4): 1191–1206.

Grover A, Benet LZ (2009) Effects of Drug Transporters on Volume of Distribution. *The AAPS Journal* 11(2): 250-261.

Highfill SL, Cui Y, Giles AJ, Smith JP, Zhang H, Morse E, Kaplan RN, Mackall CL (2014) Disruption of CXCR2-mediated MDSC tumor trafficking enhances anti-PD1 efficacy. *Sci Transl Med* 6:237ra67.

Holmes WE, Lee J, Kuang WJ, Rice GC, Wood WI (1991) Structure and functional expression of a human interleukin-8 receptor.*Science* 253: 1278-1280.

Houston JB, Carlile DJ (1997) Prediction of hepatic clearance from microsomes, hepatocytes, and liver slices. *Drug Metab Rev* 29(4): 891-922.

Houston JB (2013) Prediction of human pharmacokinetics in 2013 and beyond. *Drug Metab Dispos* 41(12): 1973-1974.

Ito K, Houston JB (2005) Prediction of human drug clearance from in vitro and preclinical data using physiologically based and empirical approaches. *Pharm Res* 22(1): 103-112.

Iwatsubo T, Hirota N, Ooie T, Suzuki H, Shimada N, Chiba K, Ishizaki T, Green CE, Tyson CA, Sugiyama Y (1997) *Pharmacol Ther* 73(2): 147-171.

Jamieson T, Clarke M, Steele CW, Samuel MS, Neumann J, Jung A, Huels D, Olson MF, Das S, Nibbs RJB, et al. (2012) Inhibition of CXCR2 profoundly suppresses inflammation-driven and spontaneous tumorigenesis. *J Clin Invest* 122: 3127–3144.

Kissinger JT, Garver EM, Institute for Human Genen therapy, University of Pennsylvania Philidelphia PA 19104 Jonathon D Schantz MA, Schantz JD, Coatney RW and Meunier LD (1998). A new method to collect bile and access the duodenum in conscious dogs, *Contemp Top Lab Anim Sci* 37: 1247-1253.

Lavé T, Chapman K, Goldsmith P, Rowland M (2009) Human clearance prediction: shifting the paradigm. *Expert Opin Drug Metab Toxicol* 5(9): 1039-48.

Leaker BR, Barnes PJ, O'Connor B (2013) Inhibition of LPS-induced airway neutrophilic inflammation in healthy volunteers with an oral CXCR2 antagonist *Respiratory Res* 14: 137.

Lombardo F, Obach RS, Varma MV, Stringer R, Berellini G. (2014) Clearance mechanism assignment and total clearance prediction in human based upon in silico models. *J Med Chem* 22;57(10): 4397-4405.

McGinnity DF, Soars MG, Urbanowicz RA, Riley RJ (2004) Evaluation of fresh and cryopreserved hepatocytes as in vitro drug metabolism tools for the prediction of metabolic clearance. *Drug Metab Dispos* 32: 1247–1253.

Morton JP (2016) CXCR2 Inhibition Profoundly Suppresses Metastases and Augments Immunotherapy in Pancreatic Ductal Adenocarcinoma. *Cancer Cell*, 29(6): 832–845.

Mukaida N (2003) Pathophysiological roles of interleukin-8/CXCL8 in pulmonary diseases. *Am J Physiol Lung Cell Mol Physiol* 284: 1566–1577.

Murphy PM, Tiffany HL (1991) Cloning of complementary DNA encoding a functional human interleukin-8 receptor. *Science* 253: 1280-1283.

Nicholls DJ, Wiley K, Dainty I, MacIntosh F, Phillips C, Gaw A, Kärrman Mårdh C (2015) Pharmacological Characterization of AZD5069, a Slowly Reversible CXC Chemokine Receptor 2 Antagonist *J. Pharm. Exp. Ther*. 353(2): 340-350.

Obach RS, Reed-Hagen AE (2002) Measurement of Michaelis constants for cytochrome P450-mediated biotransformation reactions using a substrate depletion approach. *Drug Metab Dispos* 30: 831−837.

Obach RS, LaChapelle EA, Brodney MA, Vanase-Frawley M, Kauffman GW, Sawant-Basak A (2016) Strategies toward optimization of the metabolism of a series of serotonin-4 partial agonists: investigation of azetidines as piperidine isosteres. *Xenobiotica* 46(12): 1112-1121.

Ouellet DM, Pollack GM (1995) Biliary excretion and enterohepatic recirculation of morphine-3-glucuronide in rats. *Drug Metab Dispos* 23:478-484.

Pang KS, Rowland M (1977) Hepatic clearance of drugs.1: Theoretical considerations of a "well-stirred" model and a "parallel tube" model. Influence of hepatic blood flow, plasma and blood cell binding, and the hepatocellular enzymatic activity on hepatic drug clearance. *J Pharmacokinet Biopharm* 5: 625-653.

Riley RJ, Martin IJ, Cooper AE (2002) The influence of DMPK as an integrated partner in modern drug discovery. *Current Drug Metabolism* 3(5): 527-550.

Rowland M, Tozer TN (1989) *Clinical Pharmacokinetics: Concepts and Applications*, 3rd ed, Williams and Wilkins, Philidelphia.

Schuster D, Laggner C, Langer T (2005) Why drugs fail - a study on side effects in new chemical entities *Curr Pharm Des* 11: 3545–3559.

Sohlenius-Sternbeck A-K, Jones C, Ferguson D, Middleton BJ, Projean D, Floby E, Bylund J,Afzelius L (2012) Practical use of the regression offset approach for the prediction of in vivo intrinsic clearance from hepatocytes. *Xenobiotica* 42: 841–853.

Smith DA, Kerns EH (2010) The effect of plasma protein binding on in vivo efficacy: misconceptions in drug discovery. *Nat Rev Drug Discovery* 9: 929–939.

Soars MG, Grime K, Sproston JL, Webborn PJ, Riley RJ (2007) Use of hepatocytes to assess the contribution of hepatic uptake to clearance in vivo. *Drug Metab Dispos* 35: 859–865.

Steele CW, Karim SA, Leach JDG, Bailey P, Upstill-Goddard R, Rishi L, Foth M, Bryson S, McDaid K, Wilson Z, Eberlein C, Candido JB, Clarke M, Nixon C, Connelly J, Jamieson N, Carter CR, Balkwill F, Chang DK, Evans TRJ, Strathdee D, Biankin AV, Nibbs RJB, Barry ST, Sansom OJ, Morton JP (2016) CXCR2 Inhibition Profoundly Suppresses Metastases and Augments Immunotherapy in Pancreatic Ductal Adenocarcinoma. *Cancer Cell*, 29(6): 832–845.

Virtala R, Ekman A-K, Jansson L, Westin U, Cardell LO (2011) Airway inflammation evaluated in a human nasal lipopolysaccharide challenge model by investigating the effect of a CXCR2 inhibitor *Clin Exp Allergy*, 42: 590–59.

Walters I, Austin C, Austin RP, Bonnert R, Cage P, Christie M, Ebden M, Gardiner S, Grahames C, Hill S, Hunt F, Jewell R, Lewis S, Martin IJ, Nicholls D, Robinson D

(2008) Evaluation of a series of bicyclic CXCR2 antagonists. *Bioorg Med Chem Lett*,18(2): 798-803.

Waring MJ, Arrowsmith J, Leach AR, Leeson PD, Mandrell S, Owen RM, Pairaudeau G, Pennie WD, Pickett SD, Wang J, Wallace O, Weir A. (2015) An analysis of the attrition of drug candidates from four major pharmaceutical companies. *Nat Rev Drug Discov* 14(7): 475-486.

Wenlock MC, Barton P, Austin RP (2011) A kinetic method for the determination of plasma protein binding of compounds unstable in plasma: Specific application to enalapril. *J Pharm Biomed Anal* 1: 385-390.

Wenlock MC, Austin RP, Potter T, Barton P (2011) A highly automated assay for determining the aqueous equilibrium solubility of drug discovery compounds. *J Lab Autom* 16: 276-284.

Willis PA, Bonnert RV, Hunt SF, Walters IAS (2001) Novel thiazolo(4,5-d)pyrimidine compounds. Patent number: WO200125242 A1.

Figure Legends

Figure 1. Chemical development of CXCR2 antagonists from an early clinical candidate AZD8309, to AZD5069 and AZD4721 with twice and once daily dosing in human respectively.

Figure 2. The relationship between (A) plasma protein binding and rat plasma clearance and (B) rat steady state volume of distribution for AstraZeneca CXCR2 antagonists from the sulfamide (▲) and thiazolone (■) chemical series with correlation statistics. Individual compound data, chemical series and structure references are provided in the supplementary information (Supplemental Table 1).

Figure 3. Simulation highlighting the predicted effect of drug binding to plasma proteins on half-life (0.693 x Vss / CL). CL was predicted using the ‘regression line approach’ (Methods) with human hepatocyte CL_{int} set to be 1 µL/min/ million hepatocytes and

Vss was kept constant at 0.2 L/kg (unaffected by plasma protein binding). Dotted line indicates plasma protein binding (PPB) of 99.2% at T1/2 of 15 h.

Figure 4. AZD5069 plasma concentration-time profile following intravenous dosing (1mg/kg) to bile duct cannulated (red triangles) and non-cannulated (blue triangles) rats and bile duct cannulated (purple squares) and non-cannulated (green squares) dogs.

Figure 5. AZD4721 plasma concentration-time profile following intravenous dosing (1mg/kg) to bile duct cannulated (red triangles) and non-cannulated (blue triangles) rats and bile duct cannulated (purple squares) and non-cannulated (green squares) dogs.

Figure 6. Major metabolites of AZD5069 (A) & AZD4721 (B) following hepatocyte incubations in rat, dog and human and *in vivo* from rat and dog (Methods).

Figure 7. Human plasma concentration (mean ± SD) 24 h time-profile following oral administration of 120 mg AZD5069 (●), n = 6 or 150 mg AZD4721 (♦), n = 5.

Table 1. Mean, Standard Deviation, and 95 % limit for pairs of mean % free data in human, rat and dog plasma binding data in the same batch of plasma.

Species	Mean duplicate ratio	SD in duplicate ratio	95% of duplicate ratios below	*n*
Human	1.35	0.48	2.14	1077
Rat	1.25	0.30	1.74	356
Dog	1.26	0.46	1.97	248

DMD Fast Forward. Published on May 21, 2019 as DOI: 10.1124/dmd.119.087163
This article has not been copyedited and formatted. The final version may differ from this version.

Table 2. Mean, Standard Deviation, and 95 % limit for pairs of mean % free data in human, rat and dog plasma binding data in different batches of plasma.

Species	Mean duplicate ratio	SD in duplicate ratio	95% of duplicate ratios below	*n*
Human	1.60	0.61	2.60	161
Rat	1.33	0.49	2.13	58
Dog	1.55	0.46	2.30	71

DMD Fast Forward. Published on May 21, 2019 as DOI: 10.1124/dmd.119.087163
This article has not been copyedited and formatted. The final version may differ from this version.

Table 3: Pre-clinical data summary and predicted human PK for AZD5069 & AZD4721

	AZD5069			AZD4721		
CXCR2 human IL-8 binding FMAT pIC_{50} *	8.5			8.4		
Hepatocyte CL_{int} (µL/min/10^6 cells) rat / dog / human	12 / 11 / 4 (HLM CL_{int} = 14)			10 / 4 / 3 (HLM CL_{int} = 8)		
Solubility, µM	190			97		
$LogD_{7.4}$ / pKa / calculated fu_{inc}	1.7 / 5.8 / 0.8			1.9 / 5.7 / 0.8		
PPB (% free) rat / dog / human	2.4 / 2.3 / 0.59			0.42 / 0.46 / 0.11		
Blood/plasma ratio rat / dog / human	0.6 / 0.6 / 0.6			0.8 / 0.7 / 0.6		
in vivo PK	Rat	Dog	Human predictions	Rat	Dog	Human predictions
Predicted hepatic metabolic CL (mL/min/kg)	5.4	5.9	0.36	1.7	0.80	0.04
Observed CL (mL/min/kg)	4.2	6.5		2.4	0.50	
CL_{renal} (mL/min/kg)	<0.01	<0.01		<0.01	<0.01	
$CL_{biliary}$ (mL/min/kg)	0.10	0.10**		<0.01	0.04	
In vivo / *in vitro* unbound CL_{int} ***	0.76	1.2		1.4	0.6	
V_{ss} (L/kg)	0.32	1.1	0.25	0.19	0.15	0.11
t½ (h) (PO)	1.0 (2.5)	0.44 (2.6)	7.5	1.3 (2.7)	3.7 (8.4)	30
F (%)	31	48		45	82	

* Ligand binding assay described in Connolly et al. (2013).

** The dog BDC study was performed post candidate drug selection.

A summary of key pre-clinical *in vitro* and *in vivo* data is shown in Table 3. Based on IVIVE and negligible renal and biliary clearance in rat and negligible dog renal clearance (at the time of proceeding to Phase I clinical studies, no bile duct cannulated dog PK study had been performed on AZD5069), human CL was predicted to be 0.36 mL/min/kg (driven by entirely hepatic metabolism), Vss was predicted to be 0.25 L/kg (based on rat and dog unbound Vss measured in non-bile duct cannulated animals) and effective half-life was consequently predicted to be 7.5 h for AZD5069.

*** *In vivo* $CL_{int,u}$ calculated from the Well Stirred Liver Model (Pang & Roland, 1977) as follows:

$CL_{int,u} = CL_H / f_{ub} \times (1 - CL_H / Q_H)$ and *in vitro* $CL_{int,u}$ calculated as CL_{int} / fu_{inc}

DMD Fast Forward. Published on May 21, 2019 as DOI: 10.1124/dmd.119.087163

Figure 1

Thiazolone series

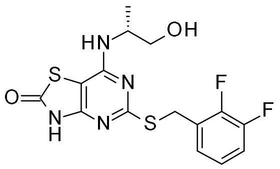

AZD8309

Sulfamide series

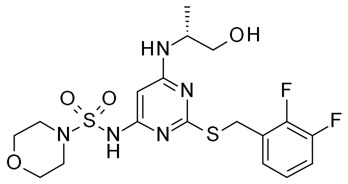

Early monocyclic sulfamide lead

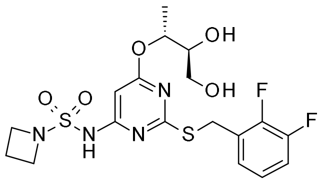

AZD5069

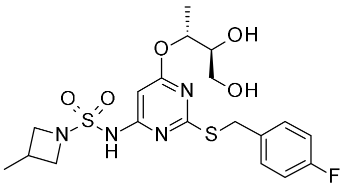

AZD4721

Figure 2

A

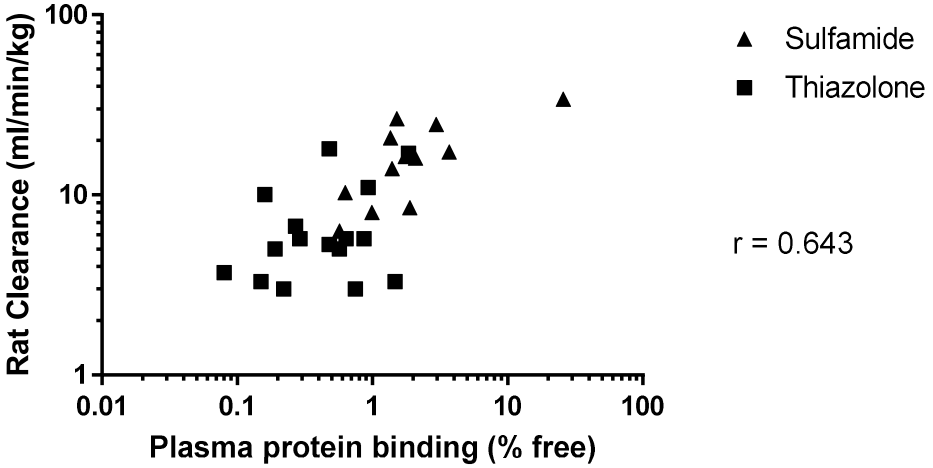
Rat Clearance (ml/min/kg)
100
10
1
0.01
0.1
1
10
100
Plasma protein binding (% free)
▲ Sulfamide
■ Thiazolone
r = 0.643

B

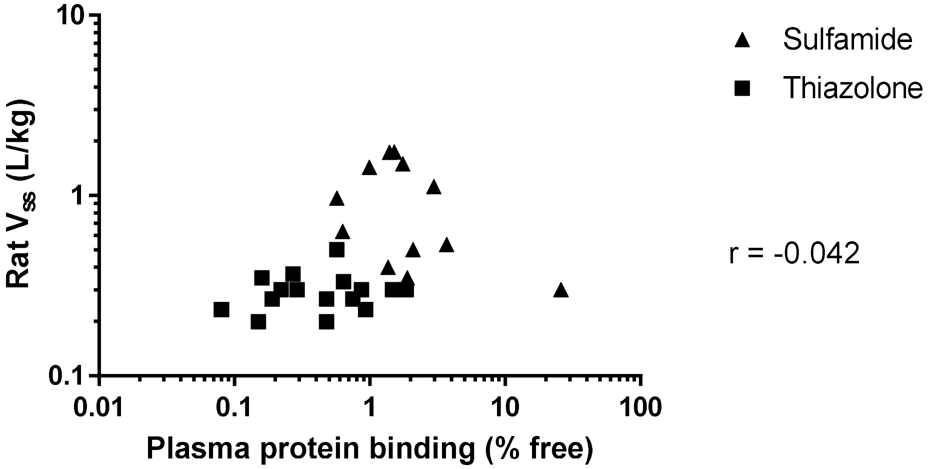
Rat V_{ss} (L/kg)
10
1
0.1
0.01
0.1
1
10
100
Plasma protein binding (% free)
▲ Sulfamide
■ Thiazolone
r = -0.042

DMD Fast Forward. Published on May 21, 2019 as DOI: 10.1124/dmd.119.087163

Figure 3

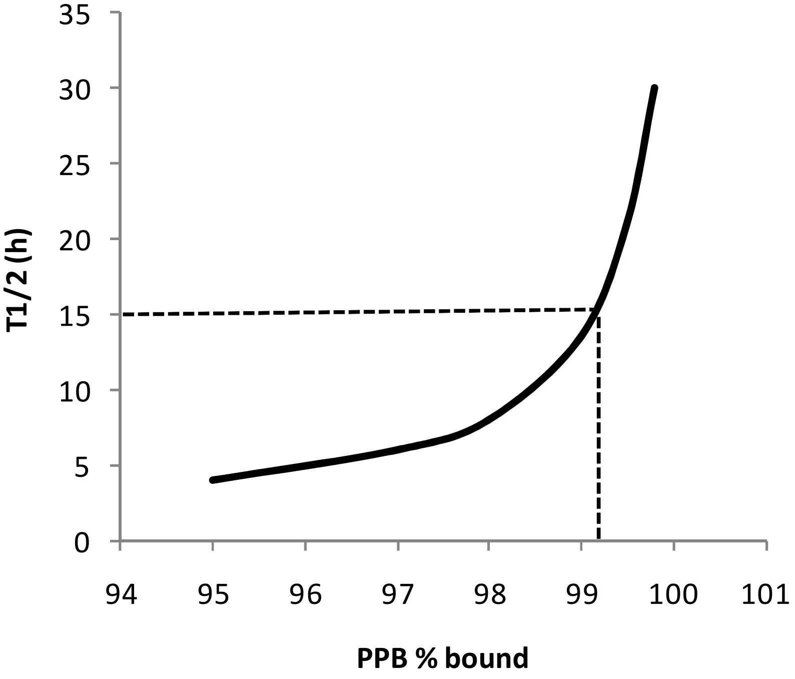

Figure 4

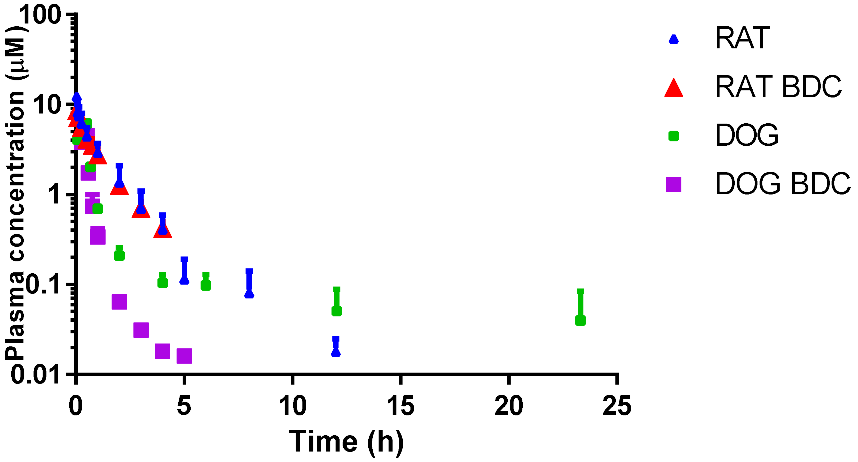
Plasma concentration (μM)
100
10
1
0.1
0.01
0
5
10
15
20
25
Time (h)
RAT
RAT BDC
DOG
DOG BDC

Figure 5

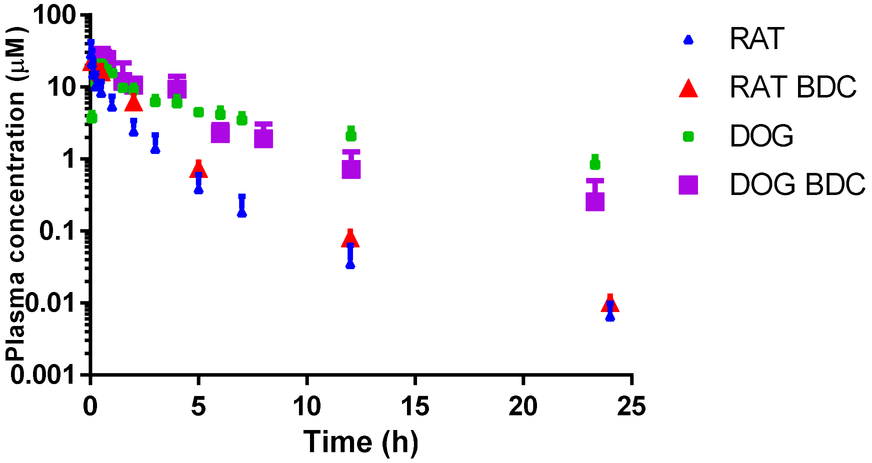
Plasma concentration (μM)
100
10
1
0.1
0.01
0.001
0
5
10
15
20
25
Time (h)
RAT
RAT BDC
DOG
DOG BDC

Figure 6

A

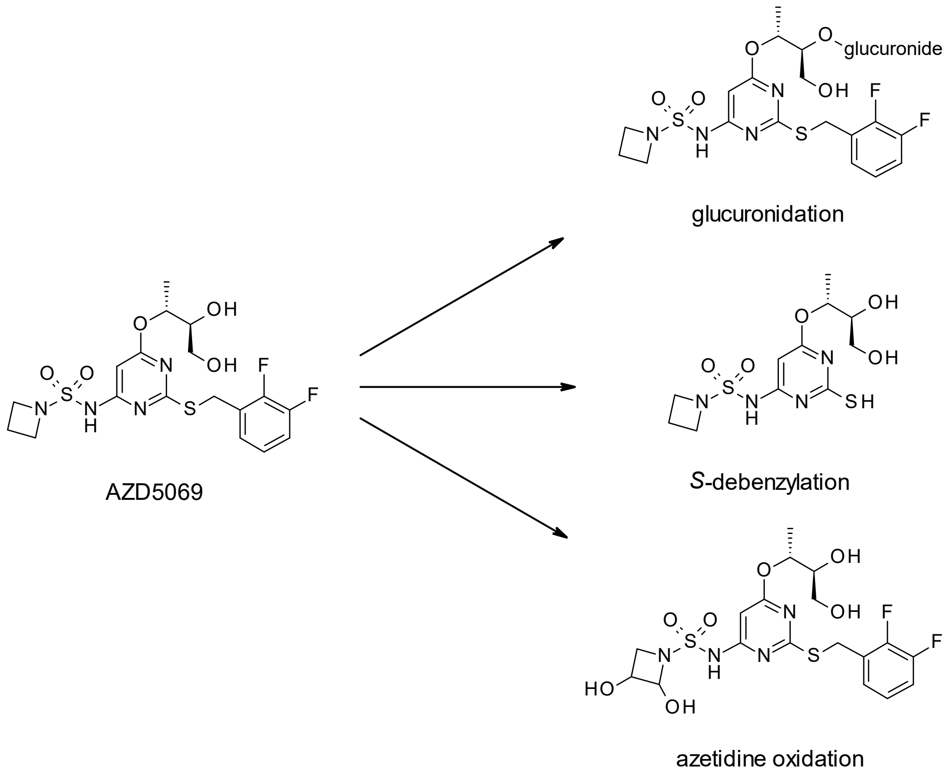
O
glucuronide
OH
F
F
O
O
S
N
N
H
N
N
S
glucuronidation
OH
OH
F
F
O
O
S
N
N
H
N
N
S
AZD5069
OH
OH
O
O
S
N
N
H
N
N
SH
S-debenzylation
OH
OH
F
F
O
O
S
N
N
H
N
N
S
HO
OH
azetidine oxidation

DMD Fast Forward. Published on May 21, 2019 as DOI: 10.1124/dmd.119.087163
This article has not been copyedited and formatted. The final version may differ from this version.

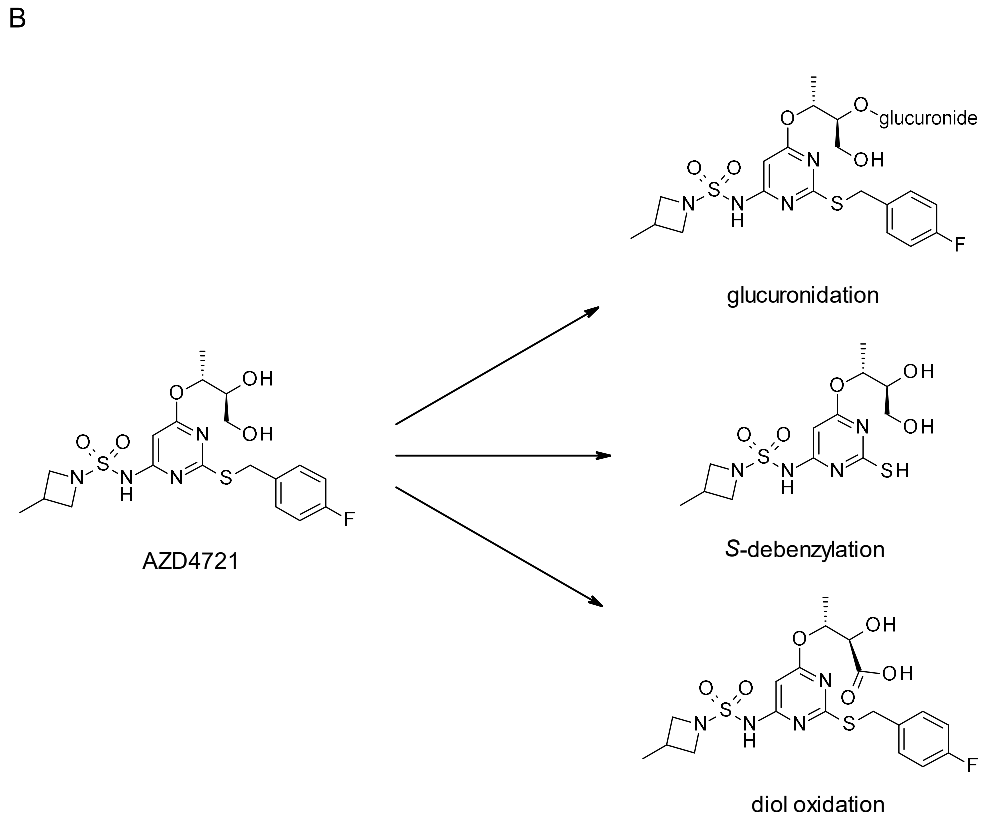
B
AZD4721
glucuronidation
glucuronide
S-debenzylation
diol oxidation

Figure 7

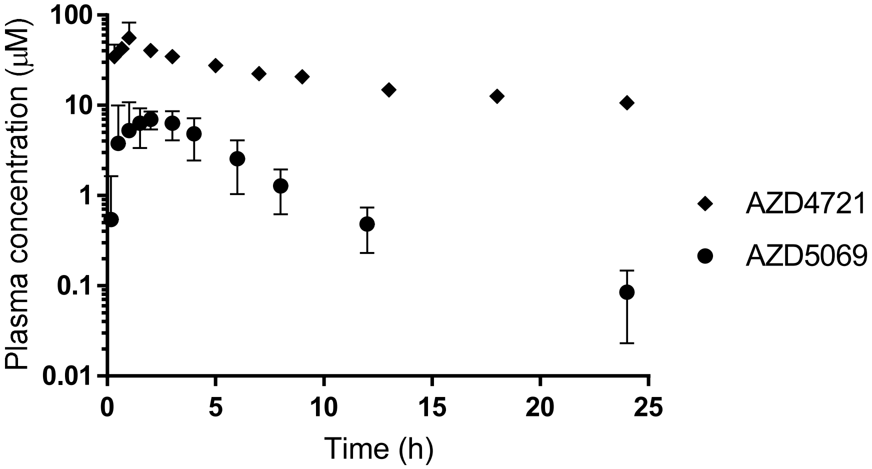
Plasma concentration (μM)
100
10
1
0.1
0.01
0
5
10
15
20
25
Time (h)
◆ AZD4721
● AZD5069

Drug Metabolism and Distribution

Plasma protein binding as an optimisable parameter for acidic drugs

Philip Gardiner, Rhona J. Cox, Ken Grime

Series	Patent	Example number in patent	CXCR2 Hu IL-8 binding pIC_{50}	plasma PB (% free)	IV PK CL (ml/min/kg)	IV PK Vss (l/kg)
AZD4721	WO 2013008002	Single example	(8.4*)	0.11	2.4	0.19
AZD5069	WO 2006024823	47	9.0 (8.5*)	0.59	4.2	0.32
AZD8309	WO 2001025242	43	9.0	0.29	5.7	0.33
sulfamide	WO 2004011443	2	7.5	2.1	16	0.5
sulfamide	WO 2004011443	27	7.9	1.5	14	1.7
sulfamide	WO 2004011443	31	8.1	3.7	17	0.53
sulfamide	WO 2004011443	36	8.2	1.5	26	1.8
sulfamide	WO 2004011443	37	8.0	1.4	21	0.4
sulfamide	WO 2004011443	39	8.4	1	8	1.4
sulfamide	WO 2004011443	41	8.5	0.57	6.3	0.97
sulfamide	WO 2004011443	106	8.4	3	25	1.1
sulfamide	WO 2004011443	107	8.0	1.8	16	1.5
sulfamide	WO 2004011443	111	8.1	0.62	10	0.63
sulfamide	WO 2004011443	131	8.2	26	34	0.3
sulfamide	WO 2004011443	138	>7.9	1.9	8.5	0.35
thiazolone	WO 2001025242	1	8.0	0.57	5	0.5
thiazolone	WO 2001025242	4	8.7	0.15	3.3	0.3
thiazolone	WO 2001025242	7	8.6	0.75	3	0.27
thiazolone	WO 2001025242	16	8.6	0.48	5.3	0.2
thiazolone	WO 2001025242	20	7.2	0.87	5.7	0.3
thiazolone	WO 2001025242	24	8.3	1.8	17	0.3
thiazolone	WO 2001025242	27	8.3	0.48	18	0.27
thiazolone	WO 2001025242	29	8.0	0.19	5	0.27
thiazolone	WO 2001025242	32	8.8	0.16	10	0.35
thiazolone	WO 2001025242	35	8.4	0.64	5.7	0.2
thiazolone	WO 2001025242	37	8.8	0.22	3	0.27
thiazolone	WO 2001025242	44	8.9	0.082	3.7	0.4
thiazolone	WO 2001025242	45	8.0	0.93	11	0.23
thiazolone	WO 2001025242	47	8.3	0.27	6.7	0.37
thiazolone	WO 2004026880	Single example	8.2	1.5	3.3	0.3

*Updated version of binding assay.